

Real-time monitoring of angiotensin II-induced contractile response and cytoskeleton remodeling in individual cells by atomic force microscopy

Charles M. Cuerrier · Martin Benoit ·
Gaétan Guillemette · Fernand Jr. Gobeil ·
Michel Grandbois

Received: 3 July 2008 / Revised: 15 September 2008 / Accepted: 26 September 2008
© Springer-Verlag 2008

Abstract Physiological processes, occurring as a result of specific receptor stimulation, are generally assessed via molecular biology techniques and microscopic approaches with the involvement of specific molecular markers. The recent progress in experimental approaches, allowing the mechanical characterization of individual biological entities, now makes it possible to address cellular processes occurring in individual cells as a result of their stimulation by hormones. Here, we demonstrate that the atomic force microscope (AFM) can be used to mechanically probe individual cells following the activation of the angiotensin-1 receptor, a receptor well known for its role in cell homeostasis regulation. Our goal is to demonstrate that the measurement of cantilever deflection can be used to quantify in real time the mechanical and morphological cell activity associated with the activation of the receptor. By combining the AFM with time-lapse sequences of phase-contrast and confocal micrographs, we show that the angiotensin-1 receptor stimulation with 100 nM angiotensin II produces an actin-dependent contractile response with an amplitude of 262 ± 52 nm. We validated the mechanical origin of the responses by measuring the elastic modulus of the cell from indentation experiments performed at 30-s intervals. Additionally, nanoscaled height fluctuations of the

cell membrane occurring after the initial contraction response could be attributed to an increased actin cytoskeleton activity and remodeling detected by confocal microscopy. Finally, by using inhibitors for specific elements of the angiotensin-1 receptor signaling pathways, we demonstrate that AFM real-time height monitoring allows a read out of the molecular processes responsible for the cell mechanical response.

Keywords Cellular mechanical response · Cell morphology · Actin reorganization · Cytoskeleton · Signaling peptide · Angiotensin II · Atomic force microscopy

Introduction

In a large variety of physiological responses, stimulation of specific signaling pathways is involved and leads to cell contraction and/or morphological remodeling. The cytoskeleton of epithelial and endothelial cells is also central to their role as barrier in various tissues and organs [1–3]. The production of actin-mediated contractile force, in response to a wide variety of agonists, such as thrombin, aldosterone, endothelin, bradykinin, and angiotensin II (AngII), are critical in the control of blood flow and vascular permeability [4–8]. These mechanically active agonists proceed through signaling pathways involving a variety of G-protein-coupled receptor (GPCR) such as G_q , $G_{12/13}$, and $G_{i/o}$, as well as small GTPases of the Rho family [4, 9, 10]. Stimulation of G proteins is directly involved in cell contraction as a result of the phosphorylation of the myosin light chain (MLC) [11]. In addition to cell contraction, the dynamic alteration of the actin cytoskeleton is a prerequisite to cellular processes associated with extensive cell shape

C. M. Cuerrier · G. Guillemette · F. Jr. Gobeil · M. Grandbois (✉)
Département de Pharmacologie, Université de Sherbrooke,
3001, 12e Avenue Nord,
Sherbrooke, QC J1H 5N4, Canada
e-mail: michel.grandbois@usherbrooke.ca

M. Benoit
Center for Nano Science,
Amalienstr.54,
80799 Munich, Germany

remodeling. Indeed, in nonmuscle cells, the Rho GTPase family is well known to regulate actin remodeling in processes leading to cell contraction [4, 9, 12], stress fiber formation [12, 13], and cell motility [14–16]. In this context, the discrimination of cellular events simultaneously causing a contraction of the cytoskeleton from those associated with dynamic actin alteration and remodeling still represents an important challenge for the understanding of cell mechanics and homeostasis regulation.

Microscopic observations in conjunction with mechanical assays, based on flexible substrates, have provided a wealth of information pertaining to cell contraction and locomotion [17–19]. More recently, nanoscaled approaches such as optical and magnetic traps [20–24], micropipette aspiration [25], shear flow [26], and atomic force microscope (AFM) [27–35] were demonstrated as powerful tools to investigate mechanical response in individual cells in various physiologically relevant contexts. The AFM was shown to be particularly suitable to cell mechanical studies as demonstrated in the monitoring of single cardiomyocytes beating amplitudes [30] and to the mechanical properties of various cellular models [36–38]. More recently, the technique was also applied to the monitoring of metabolic-driven cell membrane fluctuation in *Saccharomyces cerevisiae* [31, 32] and to the monitoring of cell pulsation in various human cells [33, 39].

In the present work, we apply the AFM to the real-time monitoring of mechanical response induced by the activation of the AngII type-1 receptor (AT₁ receptor) in individual cells. From simultaneous mechanical measurements and microscopic observations, we establish temporal relationship between the GPCR stimulation and the contractile and morphological response of the cell. The recorded mechanical responses contain information that can be interpreted in terms of actomyosin-mediated contraction and general remodeling of the cytoskeleton.

Materials and methods

Cell culture and transfection The transfection of human embryonic kidney-293 (HEK-293) cells (Qbiogene, QBI-HEK-293A cells, Carlsbad, CA, USA) with the AT₁ receptor was performed as previously described [40]. The G-418-resistant clonal cell line was maintained in DMEM supplemented with 10% heat-inactivated fetal bovine serum, 2 mM L-glutamine, 2.5 µg/ml amphotericin B, 50 IU/ml penicillin, 50 µg/ml streptomycin (Wisent, St-Bruno, QC, Canada), and 0.4 mg/ml G-418 (Gibco Life Technologies, Gaithersburg, MD, USA) at 37°C in 5% CO₂ incubator. Prior to the experiments, the cells were plated in 60-mm Petri dishes with a glass bottom coated with poly-D-lysine (MatTek Corporation, MA, USA).

Transfection of HEK-293 cells with GFP-actin was performed using FuGENE 6 transfection reagent protocol (Roche, USA). Briefly, 2 µl of FuGENE 6 was combined with 98 µl serum-free DMEM medium and then mixed with 1 µg of plasmid GFP-actin DNA (gift from Dr J-L Parent, Department of Rheumatology, Université de Sherbrooke). After 20 min of incubation at room temperature, the solution is added to cell culture Petri dish and incubated for 48 h at 37°C in 5% CO₂ incubator.

AFM measurements Our custom-made force measurement device, based on the design and operation of an AFM [39, 41], was attached to the stage of an inverted microscope (AxioVert 200, Carl Zeiss, Germany). The system uses a piezo scanner (P753.21C, Physik Instrumente, Auburn, MA, USA), equipped with a capacitive sensor with a nominal closed-loop resolution of 0.1 nm, a piezoelectric X-Y positioner (PXY 200/28 motion x, y 200 µm, Piezosystem Jena, MA, USA) and a laser source of 635 nm (OZ-2000 series, OZ Optics, USA). This arrangement allowed the precise positioning of the cantilever over the center of the cell (apical region). Soft silicon nitride cantilevers (Veeco, MLCT-AUHW, CA, USA) were cleaned with UV light ($\lambda=254$ nm, 20 W, Spectronics, Westbury, USA) for 15 min and were calibrated before and after each experiment using thermal noise amplitude analysis [42, 43]. The measured spring constants are typically found to be between 0.008 and 0.010 N/m. A typical experiment was performed as follows: A Petri dish containing HEK-293 cells was washed one time, and the growth medium was replaced with HEPES-buffered salt solution (HBSS; 20 mM Hepes at pH 7.4, 120 mM NaCl, 5.3 mM KCl, 0.8 mM MgSO₄, 1.8 mM CaCl₂, and 11.1 mM dextrose) and placed under the force measurement device. The tip of the AFM was moved over an individual cell with the help of the inverted microscope and the piezoelectric X-Y positioner. The cell approach was stopped when a contact force between the cell and the AFM tip equivalent to 200 pN was detected. This contact was maintained for at least 15 min prior to recording to ensure signal stability (flat baseline). The last fraction of this baseline was recorded for at least 5 min prior to AngII stimulation. HEK-293 cells were activated with 100 nM AngII (American Peptide, Sunnyvale, CA, USA) and, in Fig. 2e, treated with 0.5 µM latrunculin A (Sigma-Aldrich, Oakville, Ontario, Canada) for 30 min before AngII stimulation. In Fig. 4, the cells were treated with 100 µM Blebbistatin or 20 µM ML-9 for 30 min or 10 µM Y-27632 (Calbiochem, San Diego, CA, USA) for 24 h before AngII stimulation. All AFM experiments were performed at room temperature (25°C) to minimize the noise generated by the heating/cooling cycle of the temperature control device. Simultaneously, to force spectroscopy measurement, the

morphological changes of the cell were observed by phase-contrast microscopy. All micrographs were captured with a $\times 40$ phase-contrast objective, a high-sensitivity camera (AxioCam MRm, Carl Zeiss, Germany), and analyzed with AxioVision LE software to monitor morphological changes and cell area variations.

Evaluation of cell stiffness To monitor change in cell stiffness upon AT_1 receptor stimulation, cell elasticity measurements were performed on cells as previously described by others [38, 44]. As for the determination of height change, the tip of the AFM was positioned over the center of an individual cell with the help of the inverted microscope and the piezoelectric X - Y positioner. Indentation curves were recorded at 30-s intervals from 5 min before to 20 min after 100 nM AngII cell stimulation. The indentation curves were fitted with the Hertz model [44] to determine the Young's Modulus (YM). The YM is defined by $F = \delta^2 \times (2/\pi) \times [E/(1 - \nu^2)] \times \tan(\alpha)$, where F is the applied force on the cell membrane, E is the elastic modulus (kilopascal), ν is the Poisson's ratio (0.5), α is the opening angle of the AFM tip (35°), and δ is the indentation depth (300 nm in our experiments). All the experiments were performed with an approach/retract speed of 6 $\mu\text{m/s}$.

Confocal microscopy The actin cytoskeleton reorganization of cells expressing GFP-actin was analyzed from confocal microscopy micrographs. HEK-293 cells, grown on 60-mm glass bottom Petri dishes, were washed one time, and the growth medium was replaced with HBSS. The cells were examined with a scanning confocal microscope (FLUOVIEW FV1000, Olympus, PA, USA) using a $\times 40$ oil-immersion objective. GFP-actin was excited with a wavelength of 488 nm, and its emission was recorded at 505 nm. Micrographs were obtained for 15 optical sections of 1 μm for the observation from the basal (Fig. 2a) to the apical (Fig. 2c) sections of the cells. For the transverse view of the cells, 55 optical sections of 250 nm (Fig. 2b) at 15-s intervals were recorded before and after stimulation with 100 nM AngII. The time to achieve one xyz stack was 15 s. The resulting micrographs sequence was analyzed using Image-Pro Plus software to measure cell volume and to obtain apical, basal, and transversal views of cell actin distribution (MediaCybernetics, MD, USA).

Statistics In Fig. 4e, data are shown as mean value \pm standard error of the mean (SEM). To determine significance of differences ($p < 0.05$), we used an analysis of variance between the groups and a post Hoc (Dunnett correction) to compare each mean with the control group.

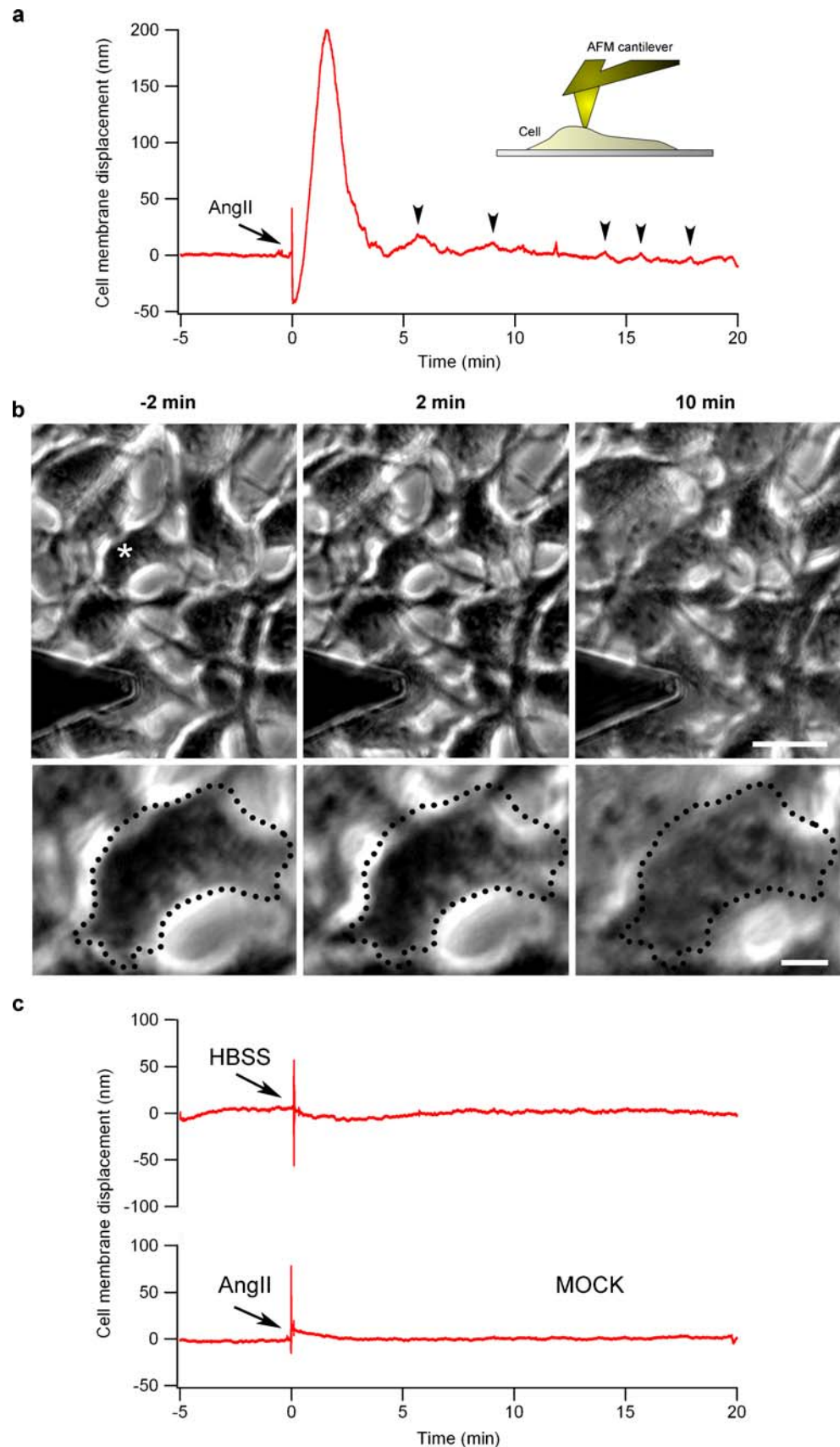
Results

Angiotensin-II-dependent contraction of individual cells measured by AFM

In this study, we use the AFM to mechanically monitor the activation of individual HEK-293 cells transfected with the AngII receptor AT_1 as published previously [45]. These cells have been previously demonstrated to respond to AngII with optical microscopy [46] and by monitoring of the intracellular calcium [47]. In Fig. 1, we combined the AFM with phase-contrast microscopy to characterize the cellular response associated with the activation of the AT_1 receptor by AngII. To record in real time the mechanical response induced by AT_1 receptor activation, an AFM force transducer with a tip of about 50 nm in radius was allowed to contact the cell surface with a force corresponding to approximately 200 pN. The AFM tip was precisely positioned over the center (apical region) of an individual cell (see insert in Fig. 1a) to minimize variation in the cellular response that could be associated to the diverse geometry observed throughout the cell surface.

Figure 1a is a typical AngII-induced cellular response detected by the AFM cantilever and plotted as cell membrane displacement (nanometer) as a function of time (minutes). In a typical experiment, the baseline prior injection of AngII is recorded for at least 5 min to ensure thermal and mechanical stability. The contact of the cell with the AFM prior of the experiment did not lead to detectable remodeling or morphology changes. At this point, the signal measured is characterized by an averaged height fluctuation of 0.70 ± 0.07 nm, corresponding to 7.0 ± 0.7 pN, as measured by averaging the AFM height data. This result is on the same order of magnitude as the typical noise of the cantilever. Immediately after the stimulation by 100 nM AngII, a cell membrane displacement of 262 ± 52 nm ($n=6$) is observed as a result of the cell pushing against the cantilever, thus developing a positive force against the tip. In order to clarify the origin of the AFM signal, we simultaneously recorded a time sequence of phase-contrast micrographs. The comparison of the cell morphology before (-2 min) and at the maximum of the height signal (~ 2 min) shows an unambiguous contraction of the cell bodies that we relate to the AT_1 receptor stimulation (see dotted lines in Fig. 1b, bottom image row). The extent of the contraction is assessed in Fig. 1b by the analysis of the cell area with the AxioVision software. Measurements performed on 50 cells result in an averaged area of $1,520 \pm 51$ μm^2 . When recorded at the maximum of the AFM height signal after AngII stimulation, a significant decrease ($p=0.004$) in the cells area is observed ($1,320 \pm 44$ μm^2), giving a reduction of area by approximately 12%. This result is consistent with the maximum cell membrane

Fig. 1 Simultaneous monitoring of AFM signal and phase-contrast micrograph on AT₁-transfected HEK-293 cells stimulated by AngII. **a** In a typical experiment, an AFM cantilever is allowed to contact the apical region of an individual cell with a force inferior to 250 pN (*insert*). A baseline is recorded for several minutes before the injection of 100 nM AngII (0 min). The cell mechanical response is plotted as cell membrane displacement unit as a function of time. **b** *Upper image row*: phase-contrast micrographs recorded before (-2 min) and after AngII stimulation (2 and 10 min). The micrograph at 2 min exhibits maximum contraction of the cells and corresponds to the maximum in the AFM height signal, whereas the micrograph at 10 min shows extensive spreading of the cell. *Bottom image row*: Magnified view of a cell (see asterisk at -2 min, *upper image row*) exhibiting cell body contraction as demonstrated by dotted lines at -2 min versus 2 min. Scale bars corresponds to 20 μ m (*upper image row*) and 5 μ m (*bottom image row*) **c** *Upper curve*: Control experiment in which HEK-293 cells, transfected with the AT₁ receptor, are exposed to an injection of 500 μ l of the buffer solution (HBSS) without AngII. *Bottom curve*: Control experiment were HEK-293 cells are transfected with an empty vector (without the AT₁ receptor coding sequence) are exposed to AngII (in 500 μ l HBSS). The AFM signals confirm that the cells do not respond to such treatment



displacement measured with the AFM (262 ± 52 nm). In this context, we argue that the contraction of the cell results in the elevation of the apical region of the cell. Another important feature of the AT₁ receptor-dependent cellular response is the significant change in morphology observed after the initial contractile response. Indeed, the phase-contrast micrograph recorded 10 min after AngII stimulation (Fig. 1b) clearly shows a significant spreading of the cell body as reported previously for this cellular model [46]. Interestingly, these structural changes are associated with an increased fluctuation in the AFM signal (see arrowheads in Fig. 1a) observed when comparing the signal before (−5 to 0 min) and after (5 to 20 min) the AngII stimulation. Indeed, in these time intervals, the averaged fluctuation increases from 0.70 ± 0.07 to 6.30 ± 0.46 nm in amplitude. We speculate here that this tenfold increase in the cell surface fluctuations can be interpreted as an index of cell remodeling activity.

In Fig. 1c, we present two control experiments conducted to confirm the contribution of the AT₁ receptor stimulation in the height response recorded with the AFM. As a control, HEK-293 cells transfected with the AT₁ receptor were stimulated with HBSS (vehicle for all AngII injection) to address the possibility that the injection could cause temperature-related force signal drift or shear stress cellular activation as observed in several cell types, including epithelial cells [48–50]. As for the AngII stimulation experiment, 500 μ l of HBSS was introduced with a micropipette into the Petri dish while the AFM signal was recorded. As expected, no AFM signal was detected (Fig. 1c, upper curve), nor any morphological changes were observed by phase-contrast microscopy (data not shown). In an additional control, the stimulation of MOCK HEK-293 cell (transfected with an empty vector) with 100 nM AngII (Fig. 1c, bottom curve) also generated no AFM response, thus confirming the implication of AT₁ receptor in the cell responses observed in Fig. 1a.

Actin activity in relation to AngII-induced mechanical response

To access the contribution of actin cytoskeleton in the recorded AFM signal, we use HEK-293 cells expressing the AT₁ receptor and co-transfected with GFP-actin to generate confocal micrographs at different times of the stimulation. From these cells, we obtain fluorescence micrograph results without the uses of conventional fluorescent probes requiring cell fixation and thus the loss of the cells response to AngII. Confocal micrographs showing different views of the cell actin at different times before and after AngII stimulation are presented in Fig. 2a and b. The confocal micrograph of the basal section (Fig. 2a) obtained prior to AT₁ stimulation shows a morphologically stable cell with

numerous actin structures [46]. A transversal confocal micrograph of a cell is presented in Fig. 2b and shows a relatively uniform distribution of the GFP-actin throughout the cell body. This transversal presentation does not easily allow for the observation of the actin structures but rather gives a general idea of the GFP-actin distribution throughout the cell body. It should be considered here that the fluorescent signal in both micrographs sets is attributed to both the f- and g-actin components of the overall actin population. Consistent with the results presented in Fig. 1, a significant contraction of the cell body (see arrowhead) is observed 2 min after AT₁ stimulation. Indeed, a careful inspection of the confocal micrographs Fig. 2a (−2 min and 2 min after the stimulation with AngII) reveals a notable reorganization of the actin content toward the cell body center, which is consistent with a contractile response of the cell. In addition, the transverse view at 2 min shows an increase in actin content at the apical region of the cell (Fig. 2b, arrowhead at 2 min), which is consistent with the height increase observed in the AFM signal. Confocal microscopy of GFP-actin in the late phase of the stimulation demonstrates an extensive rearrangement of the actin structures most notably the loss of well-defined actin filaments (Fig. 2a at 10 min) and the increase in actin density at the basal region of the cell (Fig. 2b, see arrowhead at 10 min). This reorganization of the actin cytoskeleton is concomitant with the spreading of the cell body, and we argue that this actin relocation is responsible for a good part of the fluctuation in the AFM signal in the late phase of the stimulation. Essentially, these observations confirm the implication of the actin cytoskeleton in the fluctuating AFM signal observed in the late phase of the stimulation and in the cell spreading observed in the phase-contrast micrograph in Fig. 1b (10 min). Furthermore, the change in cell height observed through AFM monitoring following the AngII stimulation can be associated to changes in cell volume. To clarify this possibility, we measured the cell volume from confocal images stacks. We found no significant change when comparing the volume before and at 2 min after AngII stimulation ($n=8$, Table 1). We calculated a volume variation of 0.01 ± 0.13 pL, which is not statistically significant; therefore, we can assume that the cell volume remains constant in the course of our experiment.

To evaluate the movement of actin structures, directly under the region where the AFM cantilever is in contact with the cell membrane, confocal micrographs of the apical section of the cell were recorded at 1-min interval before (Fig. 2c, upper panel) and after AngII stimulation (Fig. 2c, bottom panel). On the micrographs obtained before AngII stimulation, small actin structures can be observed showing a relative positioning stability in time (Fig. 2c, upper panel). In contrast, Fig. 2c (bottom panel) shows the apical

region of a cell after 15 min of AngII stimulation. One can readily observe continual changes in the position of GFP-actin structures discernible as small fluorescent elements in the micrographs. These results suggest that subtle actin movement at the apical region of the cell could be a significant contribution to the observed fluctuations of the AFM signal as shown in Fig. 1a (see arrowheads).

To further confirm the involvement of the cytoskeleton in the recorded mechanical response, cells were pretreated with the actin depolymerizing drug latrunculin A (LatA) before their stimulation by AngII. The mechanical response, normally observed when stimulating the AT₁ receptor, was greatly abolished (Fig. 2d), which clearly establishes the essential contribution of the actin cytoskeleton in the development of the mechanical response. It should be noted here that LatA pretreatment of the cells also abolished the mechanical fluctuations observed in the late phase of the stimulation, which point toward a significant contribution of actin structures in this process.

Changes in cell morphology, related to dynamic alteration of the cytoskeleton, has been demonstrated to be associated with changes in cell elastic modulus in several studies probing cellular mechanics [37, 38]. With the AFM, the Young's modulus of cells can be estimated from indentation force curves [51]. The procedure has been recently applied to study the role of the actomyosin contractile machinery in fibroblast contraction [52]. We have used this approach to confirm that the real-time mechanical response, recorded upon cell stimulation by AngII, is associated to a change in cell stiffness. In Fig. 3, we present the results of an experiment designed to monitor changes in Young's modulus in cell stimulated with AngII. In this experiment, indentation curves (Fig. 3b) are recorded every 30 s and analyzed to produce a time course of the variation of cell elastic modulus (Fig. 3c). As expected, due to cytoskeleton reorganization, we observe a sharp increase from 969 ± 95 to $3,727 \pm 461$ Pa of the calculated Young's modulus approximately 2 min after AngII stimulation. These results are consistent with the results presented in Figs. 1 and 2 and confirm that a change in cell stiffness is a major contribution to that height change observed in real-time measurement of AngII-induced cellular response, making it a valuable procedure for probing of fast transient mechanical cellular response.

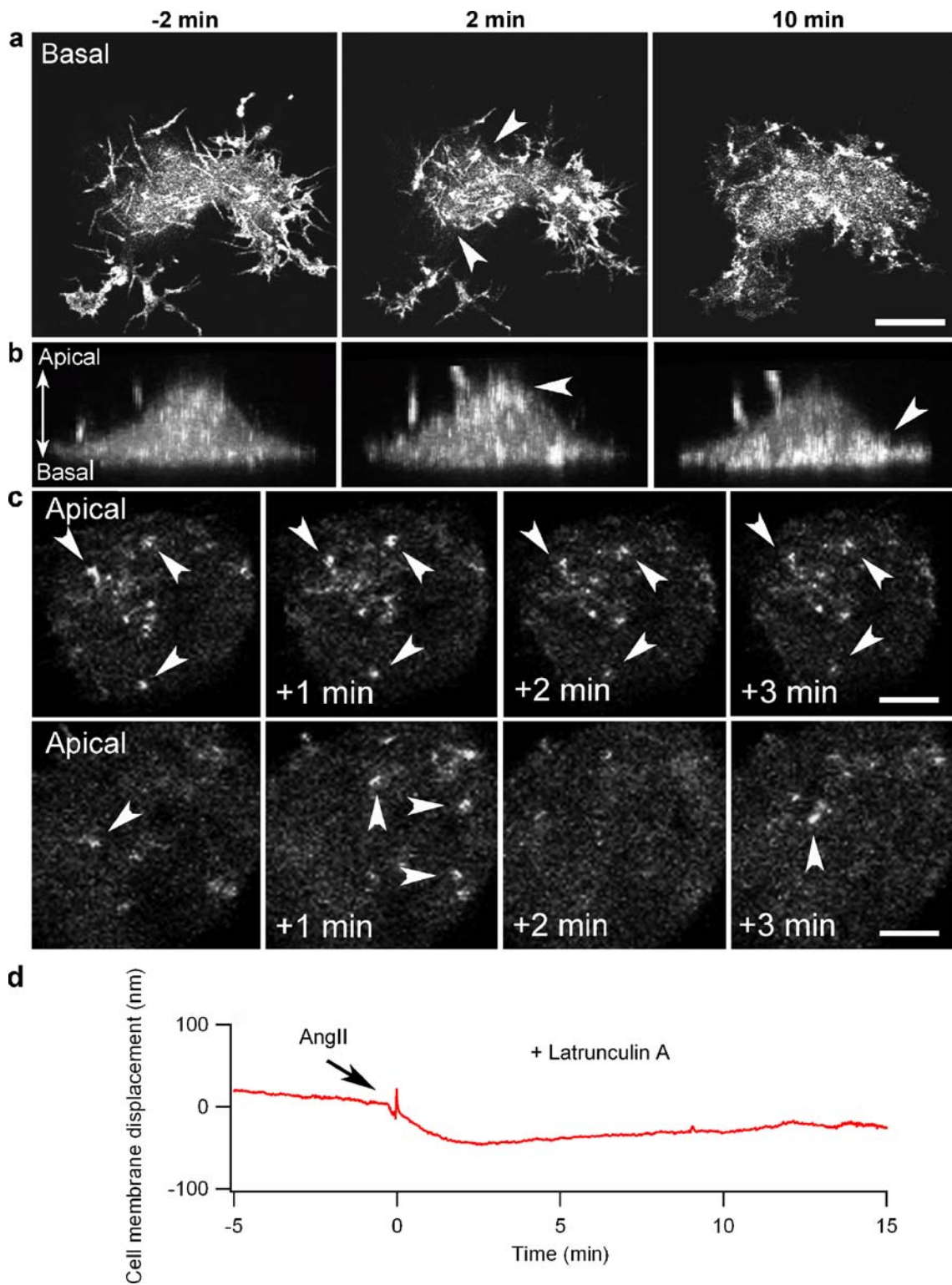
Regulatory cascade responsible for the mechanical response

In muscle and nonmuscle cells, the actomyosin system is largely involved in the regulation of contraction, motility, and actin-based cytoskeleton dynamics. In order to test the involvement of actomyosin force generation in the observed mechanical response following the stimulation of the AT₁ receptor, we pretreated the cell with the inhibitor

Fig. 2 Confocal imaging of HEK-293 cells, transfected with GFP-actin, in relation to the mechanical response measured with the AFM. **a** Confocal imaging of 1- μ m-thick section recorded in the basal region of the cell showing actin structures. Micrographs are presented at selected times before and after AngII stimulation (-2, 2, and 10 min). The *arrows* indicate the apparent contraction of the cell body. **b** Transversal view of an individual cell, constructed from 55 sections of 250 nm, before and after AT₁ receptor stimulation. The *arrows* show, respectively, the redistribution of the GFP-actin to apical and basal regions of the cell at 2 and 10 min after AngII stimulation. *Scale bar* in **a** and **b** corresponds to 10 μ m. **c-d** Relation between height fluctuation in the AFM signal and actin movement observed in confocal micrographs of the apical regions of a cell transfected with GFP-actin. The confocal micrographs correspond to a 1- μ m-thick section in the apical region of the cell recorded at 1-min time intervals before (**c**) and 15 min after (**d**) AngII stimulation. **c** The *bright spots* correspond to actin structures, which are essentially stable throughout the time sequence (see *arrowheads*). **d** The *bright spots* (see *arrowheads*) in the time sequence reflect an increased dynamical state of the actin structures. *Scale bar* in **c** and **d** corresponds to 5 μ m in confocal micrographs. **e** Monitoring of the mechanical response induced by AngII (100 nM) on HEK-293 cells pretreated with LatA (0.5 μ M). In this experiment, the cells do not react markedly compared to Fig. 1a, thus demonstrating the contribution of the cytoskeleton in the AFM signal

blebbistatin (Fig. 4a). This agent is known to inhibit myosin-II ATPase activity and lower actin-myosin affinity [53], thus interfering with the contraction mechanism. Figure 4b shows a representative mechanical response recorded with the AFM where the initial contractile response is totally abolished, which indicates that the actomyosin contractile machinery plays a prominent role in the development of the mechanical response following the stimulation of the angiotensin receptor.

The actomyosin-dependent contractile response requires the phosphorylation of the regulatory MLC on Thr-18 and Ser-19. This phosphorylation-dependent activation of MLC was previously shown to involve two alternative signaling pathways (Fig. 4a): the first involving MLCK, a kinase regulated through the G-protein G_q and the second involving the direct phosphorylation of MLC by Rho-kinase, a kinase regulated by the G_{12/13} signaling pathway. The Rho-kinase also has the capability to inactivate the MLC phosphatase (MLCP). To test whether MLCK contributes to the mechanical response detected by AFM, we pretreated the cell with an MLCK inhibitor (ML-9) prior to the stimulation. The AngII-induced mechanical response presented in Fig. 4c is similar to the one presented in Fig. 1 and indicates that the inhibition of MLCK has virtually no effect on the mechanical response of the cell. This result was confirmed by phase-contrast imaging clearly showing an important spreading of the cell after stimulation. In contrast, pretreatment of the cells with an inhibitor of Rho-kinase (Y-27632) largely diminished the initial mechanical response (Fig. 4d and e). This result points toward a main contribution of Rho-kinase in the regulation of the



mechanical response induced by AngII. Additionally, the apparent decrease in the signal fluctuation normally observed after the stimulation (6.30 ± 0.46 nm for AngII versus 2.23 ± 0.28 nm for Y-27632/AngII) and the decrease

in the spreading of the cell observed in the phase-contrast micrograph is consistent with the role of Rho-kinase in cytoskeleton remodeling. In Fig. 4e, we summarize the magnitudes of the contractile responses in the mechanical

Table 1 Evaluation of the cell volume from confocal images before and 2 min after 100 nM AngII stimulation

Cell	Before cell stimulation (pL)	2 min after AngII stimulation (pL)	Variations (pL)
1	10.21	10.31	0.10
2	6.79	6.17	-0.62
3	7.76	7.39	-0.37
4	8.65	9.09	0.43
5	8.99	9.07	0.08
6	7.18	7.62	0.44
7	7.82	7.96	0.13
8	9.35	9.24	-0.10
Mean±SEM			0.01±0.13 (-0.03%)

tests performed with the different pharmacological agents in terms of the magnitude of the initial contractile response of the cell.

Discussion

In the present study, we used a custom-built AFM, in the height and elasticity measurement mode, as a tool to the real-time monitoring of agonist-mediated cell contraction and fluctuation associated with reorganization of the actin

network in individual cells. Commercially available AFM cantilevers are used to quantify minute morphological changes occurring upon stimulation of the cell. These changes can be recorded precisely at the apical region of the cells with the help of an optical microscope for the precise positioning of the AFM tip over the cell surface. The detection of AFM height variation in individual cells was previously successfully applied to the monitoring of cardiomyocyte pulsing by Domke et al. [30]. One of their key finding was that the contractile response of the cardiomyocyte generates an elevation of the cell, which is easily detected as an increase in the AFM height signal. In the present study and in preliminary findings published earlier [45], we used an AFM cantilever positioned at the apical region of an individual epithelial cell stably expressing the AT₁ receptor to measure the mechanical response induced upon an agonistic stimulation. Stimulation of AT₁ receptor is well known to be linked to the activation of several distinct signaling pathways, including the G_q pathway (intracellular calcium mobilization and MLCK activation) and the small GTPases Rho (RhoK activation) [54, 55], which are key regulators of cell contraction and actin cytoskeleton remodeling (Fig. 4a). The main feature of the mechanical response occurs as a transient cell membrane displacement of several hundreds of nanometers in amplitude (262±52 nm) within minutes after the stimulation (Fig. 1a). In our cell line, the stimulation of the AT₁ receptors

Fig. 3 Indentation experiment performed at 30-s time intervals to evaluate the change in Young's modulus in a cell stimulated with AngII. In a typical experiment, the apical region (a) of an individual cell is indented with a force inferior to 250 pN (b), while the corresponding force trace is recorded. The data are fitted with the Hertz model [44] to derive the time course presented in c. Each point is an average of five independent experiments

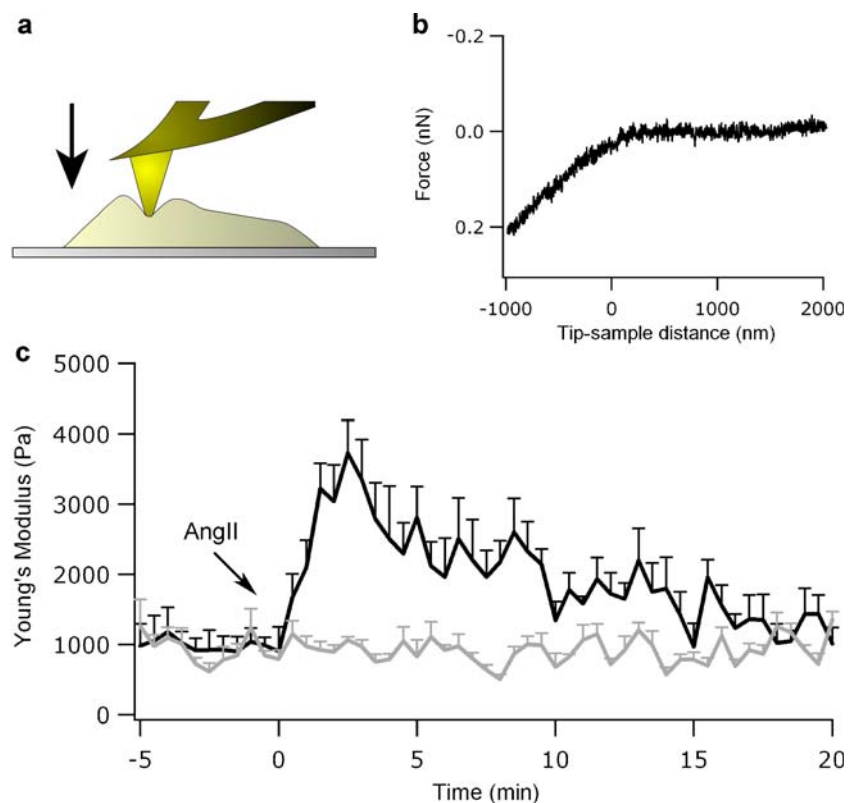
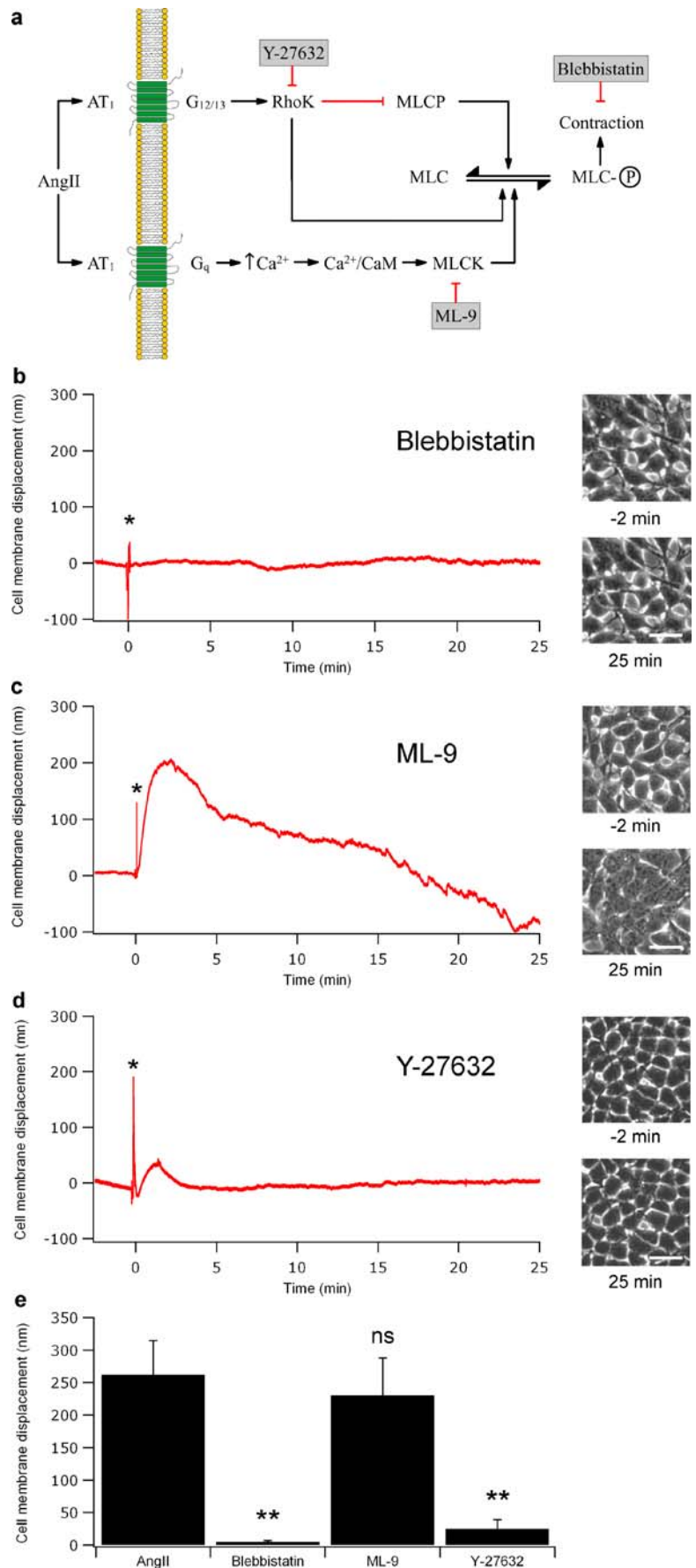


Fig. 4 Identification of the signaling pathways involved in the mechanical response induced by the activation of the AT₁ receptor. **a** Diagram presenting two independent signaling pathways known to be involved in contraction mediated by AT₁ receptor activation via its hormone AngII. The first involves G_q and ultimately leads to MLCK activation and actomyosin-based contraction, whereas the second proceeds through G_{12/13} and the activation of the kinase RhoK ultimately leading to the inhibition of the phosphatase MLCP and the direct phosphorylation of MLC by RhoK. Both events lead to actomyosin contraction. In **b**, **c**, and **d** are presented the temporal mechanical responses after treatment with inhibitor targeting the actomyosin contraction (100 μM blebbistatin), MLCK (20 μM ML-9), and RhoK (10 μM Y-27632), respectively. *Scale bar* corresponds to 50 μm in phase-contrast micrographs. **e** Summary of the magnitude of the initial contractile response in nanometer ($n=4$ to 6). $**p < 0.01$: Significantly different from AngII-stimulated cells



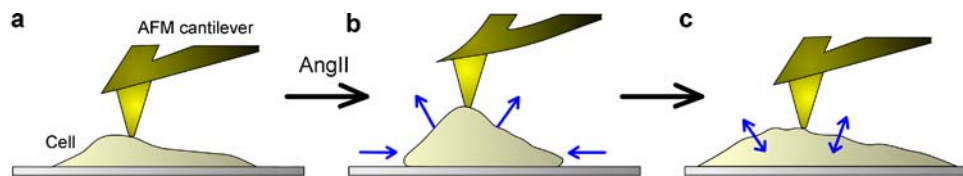


Fig. 5 Representation of the cell morphology change associated with the generation of the AFM signal. **a** Before AT_1 receptor stimulation, the AFM signal is stable and shows limited fluctuation. **b** Immediately

after the stimulation, the cell body contracts and produces a drastic increase in the AFM height signal. **c** The spreading of the cell body in the late phase of the stimulation generates the fluctuation of the signal

generates a transient contraction that could possibly play a significant physiological role at the level of various epithelial or endothelial cells. Indeed, by using the spring constant of the cantilever (0.01 N/m, nominal), we found that the contractile response of the cell can generate forces larger than 2 nN, which is sufficient to deform the surrounding extracellular matrix or to modulate fluid flow and exchange in tissue containing epithelial and endothelial cell layer. For example, lung, kidney, and blood capillary are expected to be particularly sensitive to transient contractions of epithelial and endothelial cells. Transient structural changes, with amplitude in the nanometer range, are normally difficult to visualize and to precisely quantify in real time with conventional optical microscopy technique. They are normally assessed through time-lapse micrograph sequences. The use of an AFM cantilever allows for the real-time detection of transient nanometer-scaled modification of the cell morphology and thus provides a valuable alternative for the detection of transient structural changes in cells. Here, the transient redistribution of actin structure in the apical region, observed in the confocal micrographs, was found to be consistent with the increase of the AFM height signal. More importantly, this was confirmed by the transient increase in the Young's modulus obtained from indentation curves recorded at 30-s time intervals.

When applied to cell, AFM detection relies on the direct contact of the tip with the cell surface. In principle, the sensitivity of the AFM force transducer allows for the probing of molecular movement occurring in the vicinity of the cell membrane. Such mechanical fluctuation was extensively characterized experimentally and theoretically for red blood cells [56, 57] and recently reported in various human cells [17, 29–33]. Our experiments are conducted with a sensitivity of 0.5 nm in terms of height measurement. When converted into force units, this measurement value corresponds to a force of approximately 5 pN. In the present work, we exploit the signal fluctuations to access the dynamical state of an individual cell before and after the stimulation by AngII (Fig. 1a). The averaged amplitude of the signal corresponds to cell membrane height fluctuation of 0.70 ± 0.07 nm before and to 6.30 ± 0.46 nm 10 min after the stimulation. This increase in membrane height fluctuations is correlated with an increased actin activity at the

apical region of the cells, visible in confocal micrograph of AngII-stimulated cell (Fig. 2c). Although apparently small, the difference in the fluctuating signal measured before and after the stimulation, corresponds to force exerted on the AFM tip of 7.0 ± 0.7 and 63.0 ± 4.6 pN, respectively, with occasional fluctuation reaching up to 150 pN in amplitude. Most of the fluctuations observed before the stimulation can be attributed to the thermal noise of our AFM cantilever, which is on the order of 5 pN in optimal condition. The magnitude of fluctuations observed after AngII stimulation is consistent with cellular processes involving the reorganization of the cytoskeleton. For example, single actin filament polymerization [58–60] and actin–myosin-based contraction [61–63] can generate forces of some piconewton that may add up to hundreds of piconewton when pushing in parallel on the membrane area probed by the AFM tip [64, 65]. Even though it is impossible to pinpoint the fluctuation recorded by AFM to any particular actin sub-structure, it appears that the subtle actin movement seen in the confocal micrograph at the apical region of the cell could be an important contribution to the fluctuation of the cell surface. Taken together, these results point toward the possible involvement of subtle actin movement at the apical region of cells in the increased mechanical fluctuation observed by AFM after the AT_1 receptor stimulation as seen in Fig. 1a (see arrowheads). It should be added here that other cytoskeleton elements, well known for their implication on cell mechanics, should also be taken in consideration for a possible contribution in the mechanical response observed.

Using specific inhibitors, we show that mechanical response recorded on individual cells can be used to investigate the contribution of specific signaling pathways downstream from the receptor stimulation to the overall response of the cells. First, the direct inhibition of the actomyosin contractile response by blebbistatin, which is known to influence actin–myosin binding affinity [53], produces a complete inhibition on the initial contractile response. This experiment demonstrates without ambiguity the central contribution of the actomyosin contractile machinery in the generation of the initial large amplitude mechanical response observed in our cellular model. Additionally, the use of two inhibitors for two alternative

signaling pathways leading to the phosphorylation-dependent activation of MLC allowed us to evaluate their respective contributions to the contractile response. Hence, we demonstrated that the downstream inhibition of the G_q pathway with an MLCK inhibitor (see Fig. 4a and c) had no effect on the overall mechanical response induced by the activation of the receptor AT_1 . In contrast, the inhibition of the $G_{12/13}$ pathway using a RhoK inhibitor (see Fig. 4a and d) resulted in a drastic decrease in initial contractile response as well as in an almost complete abolition of the fluctuation normally observed in the late phase of the stimulation. This result points toward a major contribution of Rho-kinase in the process. This result is consistent with the well-known multifaceted implication of Rho-kinase in actin cytoskeleton regulation and cell contraction for several cell types [4, 9, 66]. Indeed, Rho-kinase is known for its direct kinase action on both MLC and MLCP, both events leading to increased contractile activity.

In conclusion, the present study demonstrates that the AFM, in its deflection amplitude-recording mode, allows not only the precise quantification of large amplitude contractile response but also the detection of small amplitude fluctuation associated with increased cytoskeletal activity in stimulated cells (Fig. 5). Such an increase in cytoskeletal activity is often a feature of cells undergoing significant morphological changes. Promising application of the mechanical monitoring of individual cells in real time could thus be generalized to cellular processes involving sustained actin remodeling, a feature characteristic of cells undergoing significant phenotypical changes. Consequently, the AFM can provide valuable mechanistic details on signaling pathways activated by cell receptor agonists well known for their implication in mechanically relevant physiological response such as the regulation of the barrier function in epithelial and endothelial cells layers. Hence, contact AFM measurements allow for label-free and noninvasive measurements of cellular processes at high temporal and spatial resolution in living cells.

Acknowledgments We thank Eric S. Turgeon, Guillaume Arguin, and Hugo Gagnon for helpful discussion. This research was funded by the Canadian Institutes of Health Research, Natural Sciences and Engineering Research Council of Canada and a Canada Research Chair.

Competing interest statement The authors declare that they have no competing financial interests.

References

- Mehta D, Malik AB (2006) Signaling mechanisms regulating endothelial permeability. *Physiol Rev* 86:279–367
- Lee TY, Gotlieb AI (2003) Microfilaments and microtubules maintain endothelial integrity. *Microsc Res Tech* 60:115–127
- Turner JR (2006) Molecular basis of epithelial barrier regulation: from basic mechanisms to clinical application. *Am J Pathol* 169: 1901–1909
- Park JK, Lee SO, Kim YG, Kim SH, Koh GY, Cho KW (2002) Role of rho-kinase activity in angiotensin II-induced contraction of rabbit clitoral cavernosum smooth muscle. *Int J Impot Res* 14: 472–477
- Melton AC, Datta A, Yee HF Jr (2006) $[Ca^{2+}]_i$ -independent contractile force generation by rat hepatic stellate cells in response to endothelin-1. *Am J Physiol Gastrointest Liver Physiol* 290: G7–13
- Mehta PK, Griendling KK (2007) Angiotensin II cell signaling: physiological and pathological effects in the cardiovascular system. *Am J Physiol Cell Physiol* 292:C82–97
- Losel R, Schultz A, Boldyreff B, Wehling M (2004) Rapid effects of aldosterone on vascular cells: clinical implications. *Steroids* 69: 575–578
- Nobe K, Sone T, Paul RJ, Honda K (2005) Thrombin-induced force development in vascular endothelial cells: contribution to alteration of permeability mediated by calcium-dependent and -independent pathways. *J Pharmacol Sci* 99:252–263
- Emmert DA, Fee JA, Goekeler ZM, Grojean JM, Wakatsuki T, Elson EL, Herring BP, Gallagher PJ, Wysolmerski RB (2004) Rho-kinase-mediated Ca^{2+} -independent contraction in rat embryo fibroblasts. *Am J Physiol Cell Physiol* 286:C8–21
- Neves SR, Ram PT, Iyengar R (2002) G protein pathways. *Science* 296:1636–1639
- Kamm KE, Stull JT (2001) Dedicated myosin light chain kinases with diverse cellular functions. *J Biol Chem* 276:4527–4530
- Shimokawa H, Rashid M (2007) Development of Rho-kinase inhibitors for cardiovascular medicine. *Trends Pharmacol Sci* 28: 296–302
- Fukata Y, Amano M, Kaibuchi K (2001) Rho-Rho-kinase pathway in smooth muscle contraction and cytoskeletal reorganization of non-muscle cells. *Trends Pharmacol Sci* 22:32–39
- Sahai E, Olson MF, Marshall CJ (2001) Cross-talk between Ras and Rho signalling pathways in transformation favours proliferation and increased motility. *Embo J* 20:755–766
- Fukata Y, Oshiro N, Kinoshita N, Kawano Y, Matsuoka Y, Bennett V, Matsuura Y, Kaibuchi K (1999) Phosphorylation of adducin by Rho-kinase plays a crucial role in cell motility. *J Cell Biol* 145:347–361
- Chang Y, Ceacareanu B, Dixit M, Sreejayan N, Hassid A (2002) Nitric oxide-induced motility in aortic smooth muscle cells: role of protein tyrosine phosphatase SHP-2 and GTP-binding protein Rho. *Circ Res* 91:390–397
- Pletjushkina OJ, Rajfur Z, Pomorski P, Oliver TN, Vasiliev JM, Jacobson KA (2001) Induction of cortical oscillations in spreading cells by depolymerization of microtubules. *Cell Motil Cytoskeleton* 48:235–244
- Paluch E, Piel M, Prost J, Bornens M, Sykes C (2005) Cortical actomyosin breakage triggers shape oscillations in cells and cell fragments. *Biophys J* 89:724–733
- Burton K, Taylor DL (1997) Traction forces of cytokinesis measured with optically modified elastic substrata. *Nature* 385: 450–454
- Chen J, Fabry B, Schiffrin EL, Wang N (2001) Twisting integrin receptors increases endothelin-1 gene expression in endothelial cells. *Am J Physiol Cell Physiol* 280:C1475–1484
- Svoboda K, Block SM (1994) Biological applications of optical forces. *Annu Rev Biophys Biomol Struct* 23:247–285
- Hosu BG, Sun M, Marga F, Grandbois M, Forgacs G (2007) Eukaryotic membrane tethers revisited using magnetic tweezers. *Phys Biol* 4:67–78

23. Tanase M, Biaisi N, Sheetz M (2007) Magnetic tweezers in cell biology. *Methods Cell Biol* 83:473–493
24. Sterba RE, Sheetz MP (1998) Basic laser tweezers. *Methods Cell Biol* 55:29–41
25. Evans E, Yeung A (1989) Apparent viscosity and cortical tension of blood granulocytes determined by micropipet aspiration. *Biophys J* 56:151–160
26. Usami S, Chen HH, Zhao Y, Chien S, Skalak R (1993) Design and construction of a linear shear stress flow chamber. *Ann Biomed Eng* 21:77–83
27. Charras GT, Horton MA (2002) Single cell mechanotransduction and its modulation analyzed by atomic force microscope indentation. *Biophys J* 82:2970–2981
28. Sen S, Subramanian S, Discher DE (2005) Indentation and adhesive probing of a cell membrane with AFM: theoretical model and experiments. *Biophys J* 89:3203–3213
29. Rotsch C, Jacobson K, Radmacher M (1999) Dimensional and mechanical dynamics of active and stable edges in motile fibroblasts investigated by using atomic force microscopy. *Proc Natl Acad Sci U S A* 96:921–926
30. Domke J, Parak WJ, George M, Gaub HE, Radmacher M (1999) Mapping the mechanical pulse of single cardiomyocytes with the atomic force microscope. *Eur Biophys J* 28:179–186
31. Pelling AE, Sehati S, Gralla EB, Valentine JS, Gimzewski JK (2004) Local nanomechanical motion of the cell wall of *Saccharomyces cerevisiae*. *Science* 305:1147–1150
32. Pelling AE, Sehati S, Gralla EB, Gimzewski JK (2005) Time dependence of the frequency and amplitude of the local nanomechanical motion of yeast. *Nanomedicine* 1:178–183
33. Pelling AE, Veraitch FS, Pui-Kei Chu C, Nicholls BM, Hemsley AL, Mason C, Horton MA (2007) Mapping correlated membrane pulsations and fluctuations in human cells. *J Mol Recognit* 20:467–475
34. Jungmann P, Wilhelm M, Oberleithner H, Riethmuller C (2008) Bradykinin does not induce gap formation between human endothelial cells. *Pflugers Arch* 455:1007–1016
35. Kang I, Panneerselvam D, Panoskaltis VP, Eppell SJ, Marchant RE, Doerschuk CM (2008) Changes in the hyperelastic properties of endothelial cells induced by tumor necrosis factor- α . *Biophys J* 94:3273–3285
36. Hillebrand U, Hausberg M, Lang D, Stock C, Riethmuller C, Callies C, Bussemaker E (2008) How steroid hormones act on the endothelium—insights by atomic force microscopy. *Pflugers Arch* 456:51–60
37. Schafer A, Radmacher M (2005) Influence of myosin II activity on stiffness of fibroblast cells. *Acta Biomater* 1:273–280
38. Oberleithner H, Riethmuller C, Ludwig T, Shahin V, Stock C, Schwab A, Hausberg M, Kusche K, Schillers H (2006) Differential action of steroid hormones on human endothelium. *J Cell Sci* 119:1926–1932
39. Pamir E, George M, Fertig N, Benoit M (2008) Planar patch-clamp force microscopy on living cells. *Ultramicroscopy* 108:552–557
40. Auger-Messier M, Clement M, Lanctot PM, Leclerc PC, Leduc R, Escher E, Guillemette G (2003) The constitutively active N111G-AT1 receptor for angiotensin II maintains a high affinity conformation despite being uncoupled from its cognate G protein Gq/11 α . *Endocrinology* 144:5277–5284
41. Binnig G, Quate CF, Gerber C (1986) Atomic force microscope. *Phys Rev Lett* 56:930–933
42. Butt H-J, Jashke M (1995) Thermal noise in atomic force spectroscopy. *Nanotechnology* 6:1–7
43. Hutter JL, Bechhoefer J (1993) Calibration of atomic-force microscope tips. *Rev Sci Instrum* 64:1868–1873
44. Radmacher M, Fritz M, Kacher CM, Cleveland JP, Hansma PK (1996) Measuring the viscoelastic properties of human platelets with the atomic force microscope. *Biophys J* 70:556–567
45. Lamontagne CA, Cuerrier CM, Grandbois M (2008) AFM as a tool to probe and manipulate cellular processes. *Pflugers Arch* 456:61–70
46. Auger-Messier M, Turgeon ES, Leduc R, Escher E, Guillemette G (2005) The constitutively active N111G-AT1 receptor for angiotensin II modifies the morphology and cytoskeletal organization of HEK-293 cells. *Exp Cell Res* 308:188–195
47. Auger-Messier M, Arguin G, Chaloux B, Leduc R, Escher E, Guillemette G (2004) Down-regulation of inositol 1,4,5-trisphosphate receptor in cells stably expressing the constitutively active angiotensin II N111G-AT(1) receptor. *Mol Endocrinol* 18:2967–2980
48. Lopardo ML, Diaz-Sylvester P, Amorena C (2007) The effect of shear stress on the basolateral membrane potential of proximal convoluted tubule of the rat kidney. *Pflugers Arch* 454:289–295
49. Carattino MD, Sheng S, Kleyman TR (2004) Epithelial Na⁺ channels are activated by laminar shear stress. *J Biol Chem* 279:4120–4126
50. Helmke BP (2005) Molecular control of cytoskeletal mechanics by hemodynamic forces. *Physiology (Bethesda)* 20:43–53
51. Radmacher M (2007) Studying the mechanics of cellular processes by atomic force microscopy. *Methods Cell Biol* 83:347–372
52. Martens JC, Radmacher M (2008) Softening of the actin cytoskeleton by inhibition of myosin II. *Pflugers Arch* 456:95–100
53. Kovacs M, Toth J, Hetenyi C, Malnasi-Csizmadia A, Sellers JR (2004) Mechanism of blebbistatin inhibition of myosin II. *J Biol Chem* 279:35557–35563
54. Inagami T, Kambayashi Y, Ichiki T, Tsuzuki S, Eguchi S, Yamakawa T (1999) Angiotensin receptors: molecular biology and signalling. *Clin Exp Pharmacol Physiol* 26:544–549
55. de Gasparo M, Catt KJ, Inagami T, Wright JW, Unger T (2000) International union of pharmacology. XXIII. The angiotensin II receptors. *Pharmacol Rev* 52:415–472
56. Gov NS, Safran SA (2005) Red blood cell membrane fluctuations and shape controlled by ATP-induced cytoskeletal defects. *Biophys J* 88:1859–1874
57. Tuvia S, Almagor A, Bitler A, Levin S, Korenstein R, Yedgar S (1997) Cell membrane fluctuations are regulated by medium macroviscosity: evidence for a metabolic driving force. *Proc Natl Acad Sci U S A* 94:5045–5049
58. Footer MJ, Kerssemakers JW, Theriot JA, Dogterom M (2007) Direct measurement of force generation by actin filament polymerization using an optical trap. *Proc Natl Acad Sci U S A* 104:2181–2186
59. Pollard TD (1986) Assembly and dynamics of the actin filament system in nonmuscle cells. *J Cell Biochem* 31:87–95
60. Berro J, Michelot A, Blanchoin L, Kovar DR, Martiel JL (2007) Attachment conditions control actin filament buckling and the production of forces. *Biophys J* 92:2546–2558
61. Finer JT, Mehta AD, Spudich JA (1995) Characterization of single actin–myosin interactions. *Biophys J* 68:291S–296S discussion 296S–297S
62. Takagi Y, Homsher EE, Goldman YE, Shuman H (2006) Force generation in single conventional actomyosin complexes under high dynamic load. *Biophys J* 90:1295–1307
63. Ishijima A, Kojima H, Higuchi H, Harada Y, Funatsu T, Yanagida T (1996) Multiple- and single-molecule analysis of the actomyosin motor by nanometer–piconewton manipulation with a micro-needle: unitary steps and forces. *Biophys J* 70:383–400
64. Prass M, Jacobson K, Mogilner A, Radmacher M (2006) Direct measurement of the lamellipodial protrusive force in a migrating cell. *J Cell Biol* 174:767–772
65. Marcy Y, Prost J, Carlier MF, Sykes C (2004) Forces generated during actin-based propulsion: a direct measurement by micromanipulation. *Proc Natl Acad Sci U S A* 101:5992–5997
66. Samarin SN, Ivanov AI, Flatau G, Parkos CA, Nusrat A (2007) Rho/ROCK-II signaling mediates disassembly of epithelial apical junctions. *Mol Biol Cell* 18(9):3429–3439